



Coastline change in Port Beach (Western Australia) from 1988 to 2022

Seminar Paper Analysis and Modelling

Department of Geoinformatics, Paris Lodron University

supervised by Professors.

Hannah Lucille Augustin, Zahra Dabiri, Stefan Lang, Dirk Tiede

presented by

María Paula Rodríguez Navarrete

July 29th, 2023

Abstract

Historical coastline movement data is essential for effective coastal planning and management as it provides valuable insights into erosive or accretion trends and aids in identifying erosion hotspots for prioritizing mitigation measures. While aerial photography is commonly used for coastline extraction, it often incurs high costs, limited historical imagery archives, and spatial coverage. Addressing this challenge, Krause et al. (2021) proposed a comprehensive methodology that leverages the open and free Landsat ARD products of the DEA datacube to identify and extract coastlines along the Australian coastline. The approach incorporates the MNDWI index for land-water distinction, tide modelling based on the FES2014 model, composites to reduce imagery noise, and subpixel extraction of coastlines. The current study applies this methodology to map the coastlines of Port Beach, Western Australia, from 1988 and 2022 with a primary focus on identifying coastal change patterns and calculating rates. Results indicate a predominant erosive behavior, with higher coastline change and erosion rates observed near Rous Head Harbour in the south, gradually decreasing northwards towards Leighton Beach. The calculated erosion rate near the Harbour was -1.949 m/year, reducing to -0.424 m/year near Leighton Beach. Validation with the DOT coastlines dataset extracted through photogrammetry showed agreement in trends and rates, confirming the proposed method's suitability for analyzing long-term coastal changes.

Keywords: Coastlines extraction, Digital Earth Australia (DEA) datacube, Analysis Ready Data (ARD), Landsat, Coastal change

Contents

Abstract	2
Contents	3
Figures and Tables	4
Abbreviations.....	5
Introduction.....	6
Study Area	8
Materials and Methods	10
A. DEA Sandbox.....	10
B. Coastal Erosion Workflow proposed by Krause et al. (2021)	10
1) Load Cloud Masked Landsat Imagery	10
2) Calculate Normalized Difference Water Index (MNDWI)	12
3) Model Tide Heights	12
4) Filter Landsat Images by Tide Height.....	13
5) Combine tidally-masked MNDWI observations into annual median composites	14
6) Extract coastlines vectors from imagery.....	14
Results	15
A. Coastline movement.....	15
B. Erosion and progradation rates	16
C. Validation.....	17
Discussion	20
Conclusion and Outlook	21
Data Availability	22
References	22

Figures and Tables

Fig. 1 a) Location of Study Area b) Port Beach relevant infrastructure.....	8
Fig. 2 Six main steps in Krause et al. (2021) methodology.	11
Fig. 3 Comparison of coastline position in Roebuck Bay (Western Australia) at different tide heights, illustrating significant variations.	12
Fig. 4 Scatter plot of FES2014 model-derived tide height values (y-axis) plotted against the corresponding year (x-axis) for satellite images in the dataset.	13
Fig. 5 Total coastline displacement (in meters) for Rous Head Harbour and Zones A, B & C over the period from 1988 to 2022.	16
Fig. 6 Erosion rates in Zones A, B and C derived from the slope of linear regression models.	17
Fig. 7 Position of vegetation line for accreting and eroding beaches.....	18
Fig. 8 Comparison of erosion trends and coastlines position between the DEA Study Coastlines Dataset and the DOT Validation Coastlines Dataset.	19
 Table 1 Key human interventions associated with Port Beach.	 9
Table 2 Description and name of used Landsat ARD products available within the DEA datacube.	10
Table 3 Geographical coordinates (EPSG: 4326) of chosen reference points per zone utilized for coastline movement and erosion rates calculation.	15
Table 4 Geographical coordinates (EPSG: 4326) of the selected reference points from both the Study Dataset and DOT Coastlines dataset, used for comparison and validation purposes.....	18
Table 5 Slope and Standard Error obtained from linear regression analyses for selected reference points in both the Study Coastlines Dataset and the DOT Validation Coastlines Dataset.	19

Abbreviations

AMSL	Above Mean Sea Level
ARD	Analysis Ready Data
DEA	Digital Earth Australia
DOT	Department of Transport, Western Australia
DPI	Department for Planning and Infrastructure, Western Australia
FES2014	Finite Element Solution 2014
MIR	Mid-Infrared
MNDWI	Modified Normalized Difference Water Index

Introduction

The coastline, which marks the contact line between land and water at a given moment in time (Naji & Tawfeeq, 2011), is a dynamic and intricate feature of the Earth's surface. It serves as a crucial indicator of the ongoing erosive or accretion processes occurring along the coast. When the coastline moves landward over time, it indicates erosive processes, involving the removal of materials from the coast. Conversely, when the coastline advances seaward over time, it suggests accretion processes, with material deposition and land gain (Gibb, 1978). These changes in the coastline are influenced by various natural factors such as wave action, tides, storm surges, and near-shore circulation (Pandian et al., 2009). Additionally, human activities can significantly impact coastline processes, particularly by altering sediment supply, through actions like dredging, installation of protective structures like breakwaters, removal of backshore vegetation, or reclamation of near-shore areas (Berger & Iams, 1996).

Tracking long-term coastline variability, spanning over a year, is therefore of utmost importance for effective coastal management. It enables scientists, managers, and policy makers to discern trends of erosion or accretion, identify vulnerable areas experiencing erosion (erosion hotspots), and determine preventive measures required to mitigate risks. For this purpose, remote sensing images offer a multitude of advantages. They facilitate continuous monitoring of coastline positions over time due to extensive data records, the availability of repeated images of the same location at different times, and near-global coverage of the Earth's surface (Pardo-Pascual et al., 2012). The Landsat program, for instance, boasts the longest archive of medium resolution satellite images, making it a valuable resource for investigating historical coastline dynamics across various Earth regions, even in hard-to-reach coastal environments.

However, working with and analyzing large volumes of satellite images over time presents significant challenges due to their size. Moreover, making these images comparable in time demands time-consuming and labor-intensive organization and preprocessing efforts. The specific preprocessing steps may vary depending on the study case or data, but commonly involve geolocation, spatial alignment, radiometric correction, and atmospheric corrections. To address these challenges, the availability of Analysis Ready Data (ARD) offers a solution. ARD refers to satellite data that has undergone processing to meet minimum requirements and is organized in a way that enables immediate analysis with minimal additional user effort and ensures interoperability both over time and with other datasets (Lewis et al., 2018).

In the case of Australia, accessing Landsat ARD products has been greatly simplified through the Digital Earth Australia (DEA) datacube. It is an open-source and freely available datacube that efficiently manages and prepares petabytes of satellite imagery for direct analysis (Geoscience Australia, 2021a). This has proven especially valuable for coastal studies, considering that the continent's coastline stretches over 30,000 km and holds significant importance due to a high percentage of the population residing near the coast, and the coast being characterized by a mix of heavily developed and remote and inaccessible regions (Geoscience Australia, 2021b). Bishop-Taylor et al. (2021) presented a new approach for generating tide datum annual coastlines and rates of change using 32 years (1988 to 2019) of Landsat satellite data from DEA datacube. This approach combined the sub-pixel resolution waterline extraction method from Bishop-Taylor et al. (2019) with a tide modeling technique, enabling the consistent filtering of satellite imagery pixels to a standardized tide datum. Building upon this work, Krause et al. (2021) proposed a simplified six-step methodology to accurately map coastlines over time and identify areas along Australia's coastline that have experienced significant changes using the Landsat archive of the DEA datacube.

The aim of this paper is to apply Krause et al. (2021) method to evidence the change from 1988 to 2022 in the coastline position of Port beach, a popular sandy beach in the West Coast of Australia. Specifically, this study focuses on analyzing the Landsat 5, 7, 8, and 9 ARD products available within the DEA datacube to identify patterns and rates of coastal erosion or accretion at Port Beach. Furthermore, the study compares the findings with the rates calculated using the publicly available Department of Transport (DOT) Western Australia coastlines dataset, which was derived from aerial photogrammetry.

Study Area

Port Beach, located on the Western Coast of Australia at $115^{\circ}42'54''$ – $115^{\circ}44'56.4''$ east longitude, $32^{\circ}3'17.28''$ – $32^{\circ}1'44.4'$ south latitude, is a sandy beach within the City of Fremantle. Positioned between the Rous Head Harbour and Leighton Beach (**Fig. 1a**), it stretches approximately 1.5km along the coastline. Port Beach exemplifies a well-established, popular metropolitan beach where the development is in close proximity to the coastline, making it susceptible to erosion caused by coastal processes (Department for Planning and Infrastructure (DPI), 2004). Specifically, it features significant built assets that hold high value for both the local community and visitors (Seashore Engineering Pty Ltd, 2019). These assets include driveways (e.g., Rudderham and North Mole Drives), carparks, cafes, change rooms, as well as the Port Beach Road, which accommodates buried power, gas, and water pipelines (**Fig. 1b**).

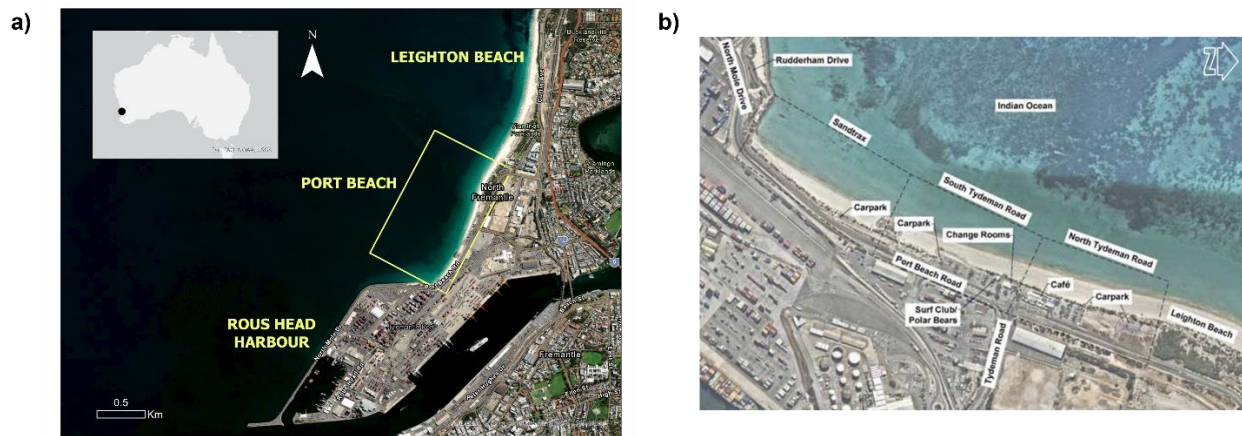


Fig. 1 a) Location of Study Area (Port Beach, Western Australia) **b)** Port Beach relevant infrastructure (m p rogers & associates pl, 2019).

Furthermore, Port Beach has a rich history characterized by extensive human intervention and 130 years of construction activities (m p rogers & associates pl, 2019). These activities have led to significant changes over time, not only in the southern harbour area but also in the configuration of the Port Beach area itself. For instance, between 1988 and 2022, notable developments occurred, including the gradual extension of Rous Head and the Inner Harbour Deepening, as outlined in **Table 1**.




Year	Description	Photograph
1989 - 1991	Inner Harbour Deepening Construction of Rous Head commercial boat harbour and seawall	 <p>1989 - Rous Head</p>
1995	Maintenance Dredging Construction of Rous Head Partial Extension and reclamation 100 m offshore.	 <p>2008 - Port Beach & Inner Harbour</p>
2009 - 2010	Inner Harbour Deepening Project Deepening of Inner Harbour, deepening of channels and construction of Rous Head Ultimate Extension.	 <p>2018 - Rous Head Ultimate Extension</p>

Table 1 Key human interventions associated with Port Beach. Modified from (m p rogers & associates pl, 2019).

Materials and Methods

A. DEA Sandbox

All the methods implemented in this study were carried out using the DEA Sandbox, a free access learning and analysis platform that offers a wide range of resources (Geoscience Australia, 2023). It provides a JupyterLab environment with pre-installed Python packages, including Open Data Cube (Dhu et al., 2019) and xarray (Hoyer & Hamman, 2017), which allow for seamless access, querying, and manipulation of the data stored within the DEA datacube. The platform also incorporates dea-tools Python package (Krause et al., 2021), which expands the functionality for loading DEA data, generating plots, conducting spatial and temporal analysis, and performing domain-specific analyses such as coastal and intertidal studies.

Moreover, the DEA Sandbox includes a collection of preloaded Jupyter notebooks (Krause et al., 2021) containing user guides and illustrative examples that showcase common analysis tasks with DEA datasets. For this study, three key notebooks, namely Coastal_erosion, Tidal_modelling.ipynb, and Animated_timeseries.ipynb, were employed and modified to align with the study's objectives.

B. Coastal Erosion Workflow proposed by Krause et al. (2021)

The workflow proposed by Krause et al. (2021) comprises six main steps as visually displayed in [Fig. 2](#).

1) Load Cloud Masked Landsat Imagery

The *load_ard* function, found in the dea-tools *datahandling* module, was applied to load the time series of cloud-masked Landsat 5, 7, 8 and 9 satellite images covering the study area over the time period spanning from 1988 to 2022. The function specifically retrieved 2007 satellite images from the DEA datacube Landsat Collection 3 products ([Table 2](#)) and organized them into a single xarray Dataset ([Fig. 2](#)).

Description	Name
Geoscience Australia Landsat 5 Thematic Mapper Analysis Ready Data Collection 3	ga_ls5t_ard_3
Geoscience Australia Landsat 7 Enhanced Thematic Mapper Plus Analysis Ready Data Collection 3	ga_ls7e_ard_3
Geoscience Australia Landsat 8 Operational Land Imager and Thermal Infra-Red Scanner Analysis Ready Data Collection 3	ga_ls8c_ard_3
Geoscience Australia Landsat 9 Operational Land Imager and Thermal Infra-Red Scanner Analysis Ready Data Collection 3	ga_ls9c_ard_3

Table 2 Description and name of used Landsat ARD products available within the DEA datacube.

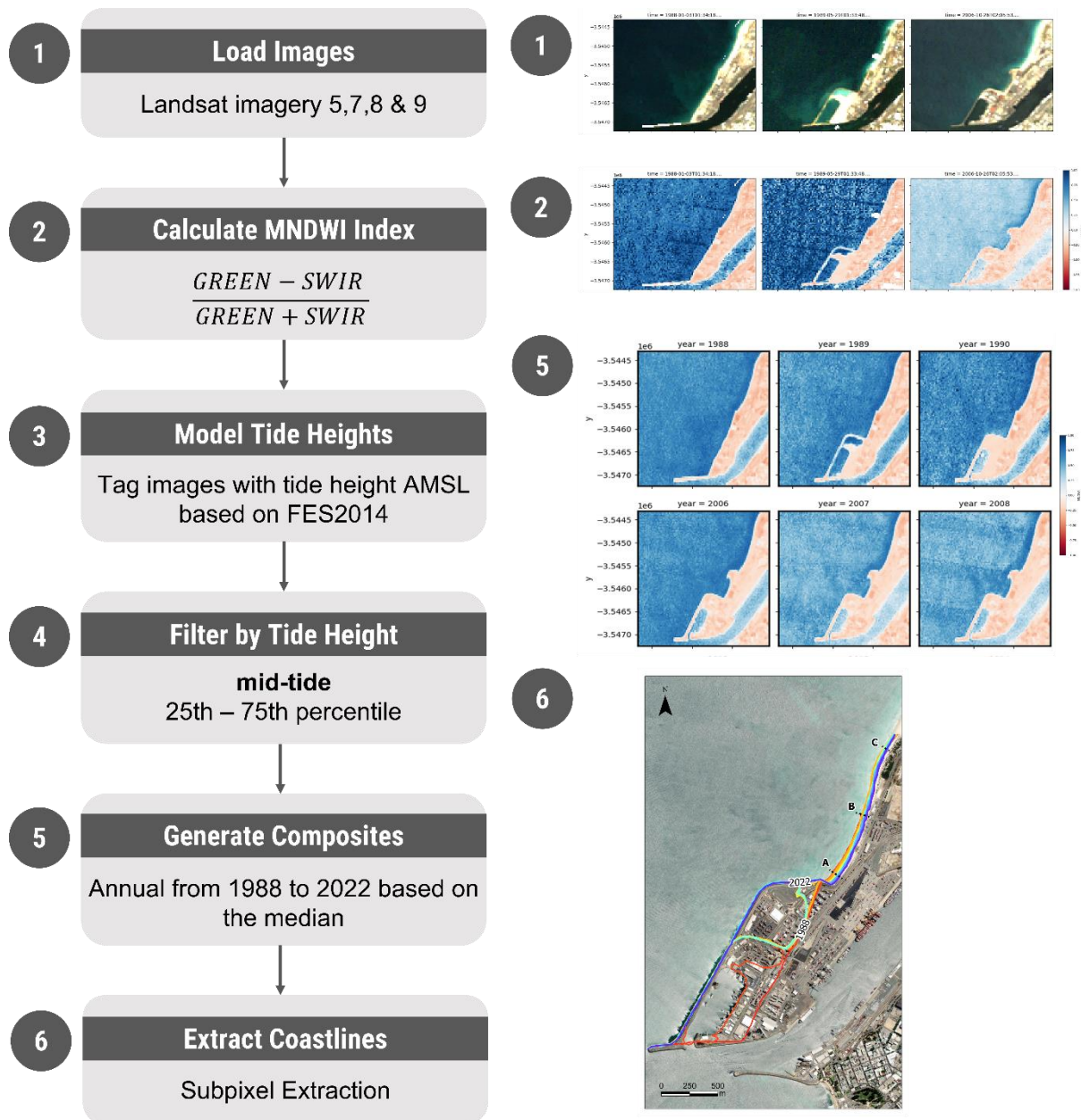


Fig. 2 Six main steps in Krause et al. (2021) methodology. Selected outputs from these steps are presented on the right side of the Figure.

The products listed in [Table 2](#) are derived by Geoscience Australia from imagery captured by Landsat 5, 7, 8, or 9 across the Australian continent. Particularly, they process Landsat data by correcting inconsistencies found along land and coastal fringes in terms of atmospheric conditions, sun position, sensor view angle, surface slope and surface aspect. As a result, these products provide accurate and standardized surface reflectance data which is essential for identifying and quantifying environmental changes over time without requiring additional corrections (Geoscience

Australia, 2019). Additionally, since the `load_ard` function automatically masked out clouds from the datasets, the analysis and examination of cloud-free pixels could directly be performed.

2) Calculate Normalized Difference Water Index (MNDWI)

To differentiate between water and land pixels in the loaded images, the MNDWI was then computed using the `calculate_indices` function from the `dea-tools` *bandindices* module, based on Xu (2006). This index utilized the ratio of Green and Mid-Infrared (MIR) bands to accurately distinguish water from non-water features. The formula for MNDWI is:

$$MNDWI = \frac{Green - MIR}{Green + MIR}$$

As suggested by Xu (2006), a threshold value of zero was applied, where positive values indicate water pixels, and low values indicate land pixels (Fig. 2)

3) Model Tide Heights

Tides are a natural phenomenon in which sea level rises and falls due to the combined effects of the gravitational forces exerted by the Moon, Sun and rotation of the Earth (Toffoli & Bitner-Gregersen, 2017). In coastal environments, tides play a significant role in determining the position of the coastline as observed in satellite imagery. During high tide, the coastline appears to be closer to the land area, while during low tide, the coastline recedes (Fig. 3). This underscores the importance of obtaining accurate tidal data corresponding to the exact time when each satellite image was captured (Krause et al., 2021).



Fig. 3 Comparison of coastline position in Roebuck Bay (Western Australia) at different tide heights, illustrating significant variations. The left image corresponds to high tide (2.52 m), while the right image shows low tide (-2.46 m).

For this purpose, the `tidal_tag` function from the coastal module of the `dea` tools package was subsequently applied. This function associated each satellite observation in the loaded time series with a tide height above mean sea level (AMSL), which is approximately equivalent to the Australian Height Datum (AHD) (Krause et al., 2021). It achieved this by getting three key characteristics of each satellite observation: the time, date of acquisition, and the geographic location of the centroid. These characteristics were then used as inputs to the Finite Element Solution 2014 (FES2014) global tidal model (Carrère et al., 2015) which ultimately calculated and returned the precise height of the tide at the exact moment and location when the satellite images in the dataset were captured.

4) Filter Landsat Images by Tide Height

To ensure temporal comparability and consistency in the observations of satellite time series, the analysis focused exclusively on images captured during mid tide. More precisely, images were kept only if their corresponding tide height fell within the range of the lowest 25th percentile to the highest 75th percentile of tide heights (Fig. 4). This approach guaranteed that all observations shared similar tidal conditions, thus enabling meaningful comparisons. In the end, out of the initial 2007 images, 1003 images met this specified condition.

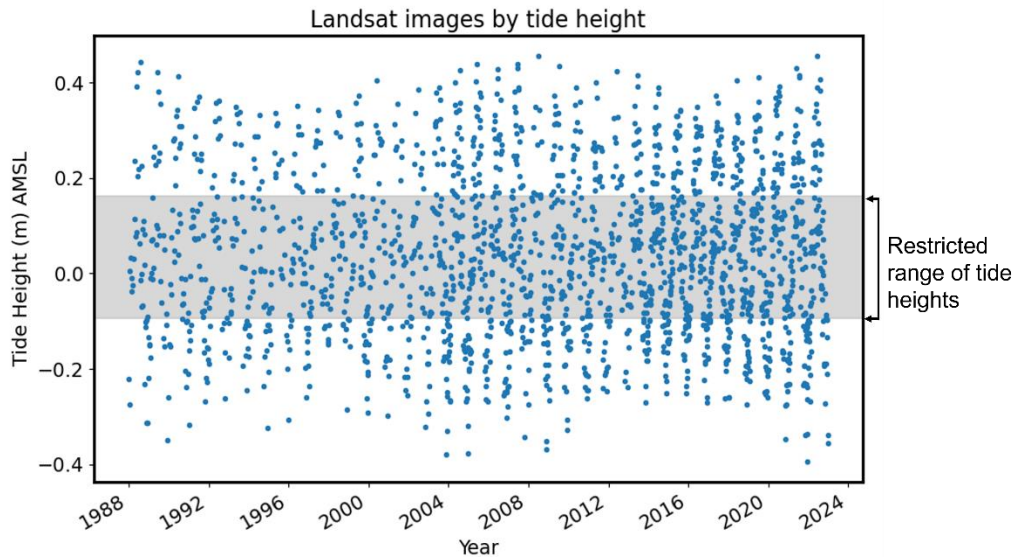


Fig. 4 Scatter plot of FES2014 model-derived tide height values (y-axis) plotted against the corresponding year (x-axis) for satellite images in the dataset. Each dot on the plot represents a satellite image, with the distribution indicating observations taken during high tide, low tide, and mid tide. The focus of this study is on images captured during mid tide, as it constitutes the range with the highest number of observations.

5) Combine tidally-masked MNDWI observations into annual median composites

As a following step, annual composites were created by combining individual MNDWI observations from the same year, using the median as the summary statistic. Unlike the mean, which can be influenced by outliers, the median provides a more reliable measure. This process resulted in a total of 35 generated composites, each representing the typical landscape appearance for a specific year from 1988 to 2022 (Krause et al., 2021) (Fig. 2).

The utilization of annual composites presents two significant advantages. First, they reduce short-term coastline fluctuations caused by events like storm surges, extreme weather, or seasonal changes, allowing for consistent monitoring and comparison of the coastal zone over time (Bishop-Taylor et al., 2021). Secondly, they minimize the impact of sun glint, unmasked clouds, and white water, all of which can degrade the quality of satellite observations. Consequently, annual composites are cleaner and nearly free of noise, enhancing their comparability and consistency across both space and time (Krause et al., 2021).

6) Extract coastlines vectors from imagery

Finally, the coastlines vectors for each annual composite were extracted using the *subpixel_contours* function found in the *spatial* module of the DEA tools package. This function utilized the MNDWI values of pixels to determine the position of the coastline. Positive values of the index indicate water, while negative values indicate land, as mentioned earlier. Consequently, pixels with values close to zero demarcated the boundary between water and land (Fig. 2).

Results

To identify the trends of coastal change in Port Beach, three designated zones (A, B, and C) were outlined in the study area. Zone A was situated closer to the Rous Head Harbour in the south, Zone C was nearer to Leighton Beach in the north, and Zone B was positioned between A and C (Fig. 5).

A. Coastline movement

Initially, the study focused only on the coastlines extracted from the first year (1988) and the last year (2022) of the study to determine the overall movement of the coastline. To do this, a reference point intersecting the 2022 coastline was chosen for each zone as listed in the Table 3. Then, using the "annual_movements" function within the vector module of the coastlines package, the distances in meters between these reference points and their respective closest points on the 1988 coastline were calculated.

Reference Point	Longitude	Latitude
Rous Head Harbour	115° 43' 53.11741" E	32° 2' 47.24966" S
Zone A	115° 44' 33.72843" E	32° 2' 23.03297"
Zone B	115° 44' 42.22923" E	32° 2' 6.37043" S
Zone C	115° 44' 49.1071" E	32° 1' 48.13436" S

Table 3 Geographical coordinates (EPSG: 4326) of chosen reference points per zone utilized for coastline movement and erosion rates calculation.

The results, as presented in the Fig. 5, indicate that the total distance changed for the coastline in the Harbour was 501.21m, while for the reference points in Zone A, B, and C, the distances were 66.14 m, 37.93 m, and 11.05 m, respectively.

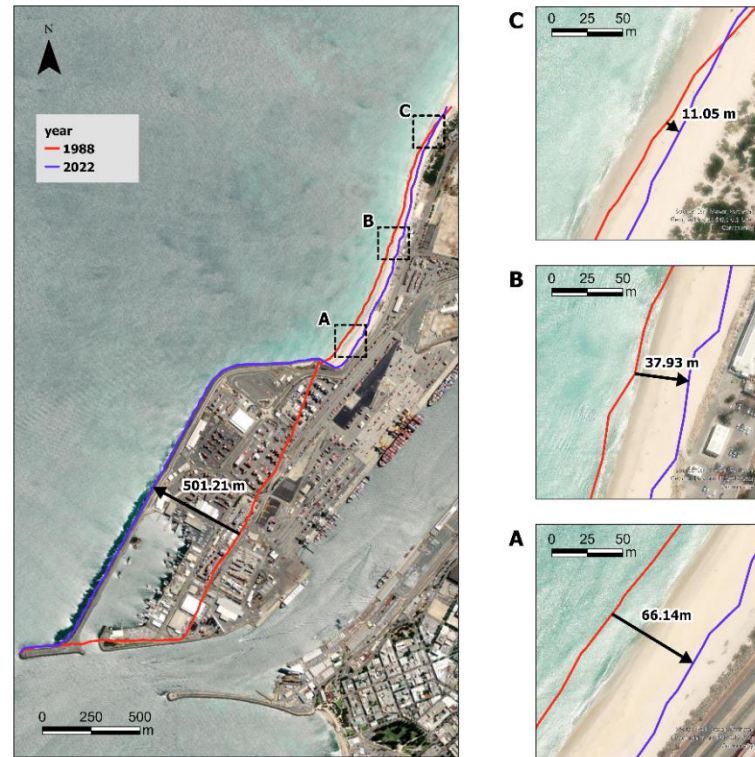


Fig. 5 Total coastline displacement (in meters) for Rous Head Harbour and Zones A, B & C over the period from 1988 to 2022

B. Erosion and progradation rates

To quantify the rates of erosion or progradation, all extracted coastlines were considered. The same reference points ([Table 3](#)) were utilized, and their distances to their nearest point on each of the other annual coastlines were calculated with the `annual_movements` function. Afterward, linear regression analyses were completed using time (years from 1988 to 2022) as the dependent variable and distances as the independent variable with the `scipy.stats` module, yielding their respective slopes and standard errors. The obtained slope was used as the approximate measure of the erosional or progradation rate of the coast at the selected points.

The obtained rates for Zones A, B, and C were -1.949 m/year, -1.176 m/year, and -0.424 m/year, respectively. These results are displayed in detail in [Fig. 6](#).

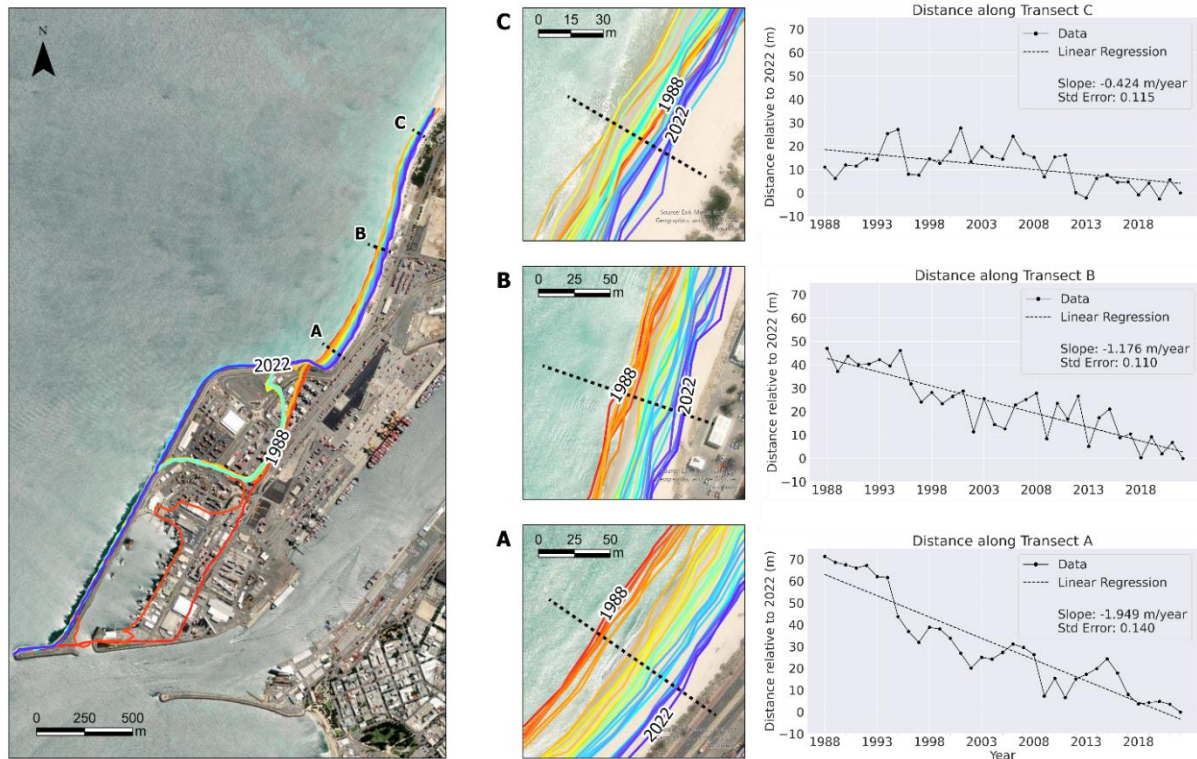


Fig. 6 Erosion rates in Zones A, B and C derived from the slope of linear regression models. These models were computed using year (ranging from 1988 to 2022) as the independent variable and the distances relative to 2022 coastline as the dependent variable.

C. Validation

DOT provides a publicly available and free polyline feature dataset on the Data WA catalog (<https://catalogue.data.wa.gov.au/dataset/coastline-movements>). This dataset comprises coastal lines captured through aerotriangulated aerial photography, covering the Western Australia coast for all decades from 1940 to 2022. The dataset employs the position of the vegetation line, which delineates the boundary between the back beach and dune toe where vegetation first appears, as an estimation of the coastline position. In cases where the beach is advancing (accreting), the dunes grow and extend towards the sea, leading to the emergence of new coastal heath beyond the existing vegetation, thereby pushing the vegetation line seaward. Conversely, when the beach is retreating (eroding), the toe of the fore dune is eroded, causing the beach to steepen, and removing vegetation, which results in the vegetation line moving landwards (Stead, 2018) (**Fig. 7**).

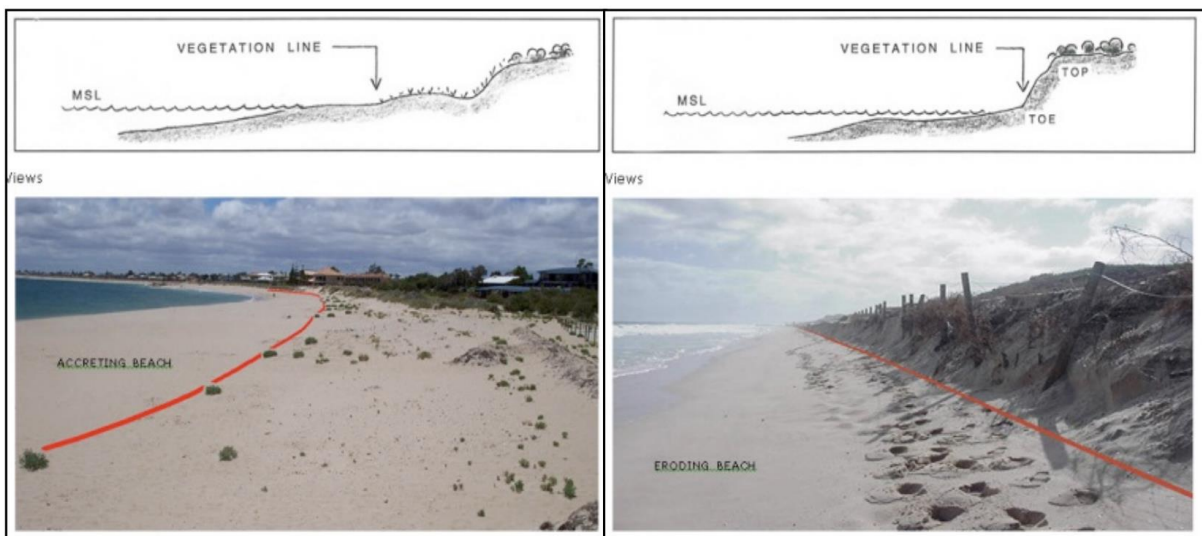


Fig. 7 Position of vegetation line for accreting and eroding beaches. Adopted from Stead (2018).

For the study area, the available data in the DOT dataset is limited until 2019. To ensure coherence in the analysis, it was necessary to take the following steps:

- Filtering the coastlines extracted in this study up to the year 2019.
- Selecting two new reference points, this time based on the 2019 coastline ([Table 4](#)).
- Calculating their distances to the rest of the coastlines and performing Linear Regression, as outlined in the previous section.

Similarly, the same procedure was repeated for the DOT coastlines, selecting reference points from the same coastal section as those chosen for the study coastlines ([Table 4](#)). The comparison of the rates obtained from both datasets is presented in the [Table 5](#) and [Fig. 8](#).

No.	DEA Study Coastlines Dataset		DOT Validation Coastlines Dataset	
	Longitude	Latitude	Longitude	Latitude
1	115° 44' 34.21981" E	32° 2' 22.38063" S	115° 44' 34.68633" E	32° 2' 22.6762" S
2	115° 44' 43.79739" E	32° 2' 0.85722" S	115° 44' 44.72558" E	32° 2' 0.84713" S

Table 4 Geographical coordinates (EPSG: 4326) of the selected reference points from both the Study Dataset and DOT Coastlines dataset, used for comparison and validation purposes.

No.		DEA Study Coastlines Dataset	DOT Validation Coastlines Dataset
1	Slope	-1.953 m/year	-1.922 m/year
	Standard Error	0.227	0.288
2	Slope	-0.818 m/year	-0.672 m/year
	Standard Error	0.186	0.161

Table 5 Slope and Standard Error obtained from linear regression analyses for selected reference points in both the Study Coastlines Dataset and the DOT Validation Coastlines Dataset.

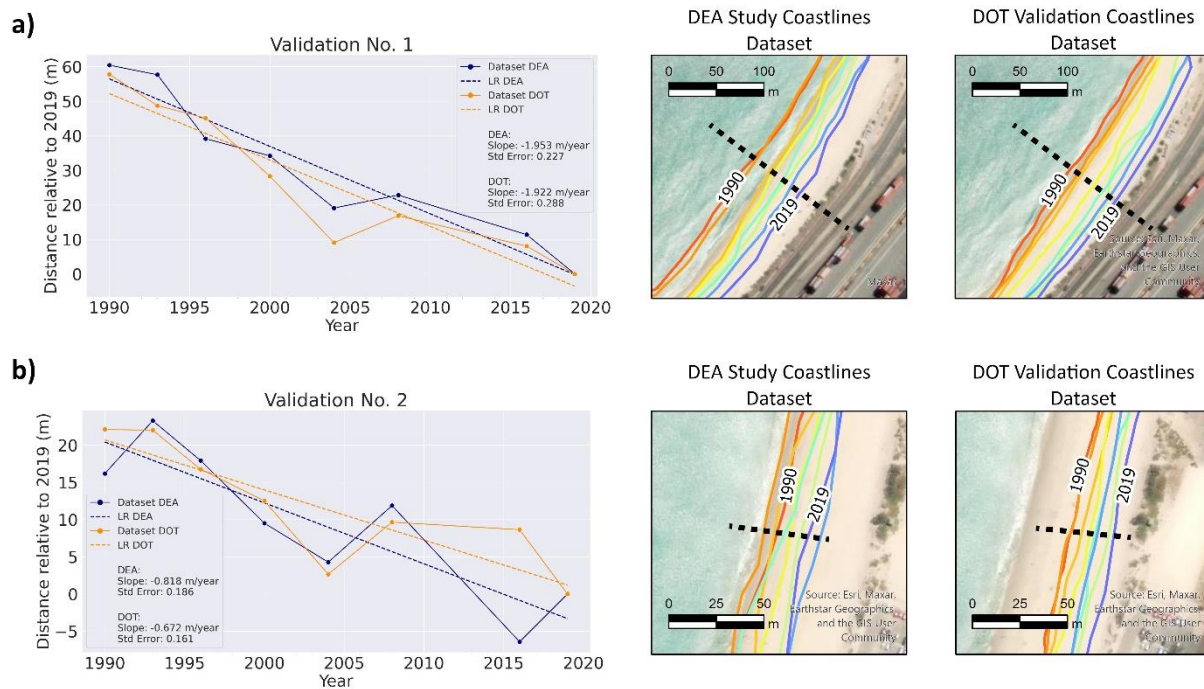


Fig. 8 Comparison of erosion trends and coastlines position between the DEA Study Coastlines Dataset and the DOT Validation Coastlines Dataset for: **a)** Reference Point 1 **b)** Reference Point 2. LR: Linear Regression

Discussion

During the study period covering from 1988 to 2022, the Rous Head Harbour coastline experienced a notable seaward movement of approximately 501m (Fig. 5). This significant shift was primarily attributed to human interventions, including the construction of a commercial boat harbor and a seawall between 1989 and 1991, as well as offshore land reclamations and extensions of Rous Head in 1995 and from 2009 to 2010. Throughout this specific section of the coastline, all observed changes were directly linked to anthropogenic activities. Meanwhile, in the outlined areas in Port Beach (A, B, and C), there was evident erosive behavior, indicating a landward shift of the coastline. Particularly, zone A, situated closer to the Harbour, experienced the most substantial erosion, with an approximate 66 m landward shift. As moving northward from A, the extent of erosion decreased, with zone B showing a displacement of approximately 38m and zone C only 11 m. Remarkably, zone C displayed a stable meeting point, with the relative position of the coastline remaining unchanged between 1988 and 2022 (Fig. 5).

The rates of erosion at Port Beach, derived from the analysis of all extracted coastlines, consistently exhibited the same erosive trend. Zone A displayed a steeper slope in the linear regression, indicating a higher erosive rate of -1.949 m/year. Conversely, as moving northward, the slope became gentler, with zone C showing a slope close to 0 of -0.424 m/year (Fig. 6). This trend of a more stable coastline towards the north was reinforced. It is essential to note that the results obtained for Port Beach do not definitively attribute the erosion patterns solely to anthropogenic intervention events in the Harbour. When examining the Distance Vs Time (years from 1988 to 2022) plots for each zone (Fig. 6), there was no Year that marked a substantial change in the slope of the regression or indicated a sudden shift in erosion rates. The slopes in all three plots remained relatively similar during the period of interest, suggesting that erosion was present both before and after the intervention events on the Harbour in the South. Therefore, it appears that other factors may also be contributing to the erosion observed in Port Beach.

Regarding the validation of results, the extracted rates in this study using DEA Landsat ARD products were found to closely match those derived from the DOT dataset at both selected reference points located in the south and north of Port Beach. Specifically, at the first reference point, the rates were -1.953 m/year using DEA Landsat data and -1.922 m/year using DOT data. Similarly, at the second reference point, the rates were -0.818 m/year with DEA Landsat data and -0.672 m/year with DOT data (Fig. 8). Despite the Landsat imagery having a coarser spatial resolution compared to the aerial imagery used for the DOT dataset, and the utilization of different methodologies for coastline extraction in both cases, the trend observed in both situations exhibited remarkable similarity.

Conclusion and Outlook

By applying the Krause et al. (2021) methodology, which leverages the Landsat ARD products of the DEA datacube, this study thoroughly mapped the coastal changes at Port Beach, Western Australia from 1988 to 2022. The main goal was to identify trends of coastal erosion or accretion and quantify the rates of change during this timeframe. The results showed that Port Beach experienced erosion throughout the entire study duration. Notably, the major changes occurred in areas closer to the Harbor in the south, while moving northward, the coastlines became more stable until they reached a point of intersection between the coastline of 1988 and 2022, indicating no significant relative change. Likewise, the rate of coastal change near the Harbor was determined to be higher compared to the vicinity of Leighton Beach in the north, where erosion rate approached zero.

Furthermore, this study demonstrated the high applicability of Krause et al. (2021) methodology in assessing long-term coastal erosion patterns. Despite utilizing Landsat data, which has a coarser resolution compared to aerial photography, the calculated erosion rates at Port Beach align closely with the rates obtained from the publicly available DOT coastlines dataset. This methodology offers valuable insights into identifying long-term coastal erosion trends, overcoming limitations such as the scarcity of historic data for specific areas and the ability to track coastal changes in hard-to-reach regions. The comprehensive methodology, which involves utilizing the MNDWI index, modeling tide height through the FES2014 model, generating annual composites, and applying subpixel contour extraction, establishes a robust framework for understanding coastal erosion trends.

Lastly, it is important to acknowledge that the causes of the observed rates in Port Beach cannot be uniquely inferred from the coastlines mapping. Although analyzing coastline changes is a necessary initial step, it is required to consider additional factors to have a comprehensive understanding of the processes at play. Integrating the findings of this study with data on wave and current action, sediment budget, and dynamics becomes essential to establish a robust and reliable conclusion regarding the primary drivers of the coastal erosion patterns in Port Beach. By doing such complementary research, it will be possible to make more informed decisions concerning coastal planning and risk management in the area, ensuring a sustainable approach to address potential challenges posed by changing coastlines.

Data Availability

The code utilized to generate the results and figures presented in this paper were posted on the following public GitHub repository: https://github.com/mariarodriguezn/Port_Beach_Coastlines

References

- Berger, A. R., & Iams, W. J. (1996). Geoindicators: assessing rapid environmental changes in earth systems. (No Title).
- Bishop-Taylor, R., Nanson, R., Sagar, S., & Lymburner, L. (2021). Mapping Australia's dynamic coastline at mean sea level using three decades of Landsat imagery. *Remote Sensing of Environment*, 267, 112734. <https://doi.org/10.1016/j.rse.2021.112734>
- Bishop-Taylor, R., Sagar, S., Lymburner, L., Alam, I., & Sixsmith, J. (2019). Sub-Pixel Waterline Extraction: Characterising Accuracy and Sensitivity to Indices and Spectra. *Remote Sensing*, 11(24), 2984. <https://doi.org/10.3390/rs11242984>
- Carrère, L., Lyard, F. H., Cancet, M., & Guillot, A. (2015). *FES 2014, a new tidal model on the global ocean with enhanced accuracy in shallow seas and in the Arctic region*.
- Department for Planning and Infrastructure (DPI). (2004). *PORT BEACH Coastal Erosion Study - Report No. 427*. <https://www.yumpu.com/en/document/read/11669786/port-beach-coastal-erosion-study-western-australian-planning->
- Dhu, T., Giuliani, G., Juárez, J., Kavvada, A., Killough, B., Merodio, P., Minchin, S., & Ramage, S. (2019). National Open Data Cubes and Their Contribution to Country-Level Development Policies and Practices. *Data*, 4(4), 144. <https://doi.org/10.3390/data4040144>
- Geoscience Australia. (2019, November 26). *DEA Surface Reflectance (Landsat 5 TM)*. <https://cmi.ga.gov.au/data-products/dea/358/dea-surface-reflectance-landsat-5-tm>
- Geoscience Australia. (2021a, February 1). *The Open Data Cube*. <https://www.dea.ga.gov.au/about/open-data-cube>
- Geoscience Australia. (2021b, June 3). *Time and Tide: Mapping Australia's dynamic coastal zone*. <https://youtu.be/giJoEumWOLY>

- Geoscience Australia. (2023). *Digital Earth Australia User Guide*. <https://docs.dea.ga.gov.au/>
- Gibb, J. G. (1978). Rates of coastal erosion and accretion in New Zealand. *New Zealand Journal of Marine and Freshwater Research*, 12(4), 429–456. <https://doi.org/10.1080/00288330.1978.9515770>
- Hoyer, S., & Hamman, J. (2017). xarray: N-D labeled Arrays and Datasets in Python. *Journal of Open Research Software*, 5(1), 10. <https://doi.org/10.5334/jors.148>
- Krause, C., Dunn, B., Bishop-Taylor, R., Adams, C., Burton, C., Alger, M., Chua, S., Phillips, C., Newey, V., Kouzoubov, K., Leith, A., Ayers, D., Hicks, A., Contributors, D. E. A., & Chua, S. (2021). *Digital Earth Australia notebooks and tools repository*. Geoscience Australia, Canberra. <https://doi.org/10.26186/145234>
- Lewis, A., Lacey, J., Mecklenburg, S., Ross, J., Siqueira, A., Killough, B., Szantoi, Z., Tadono, T., Rosenavist, A., Goryl, P., Miranda, N., & Hosford, S. (2018). CEOS Analysis Ready Data for Land (CARD4L) Overview. *IGARSS 2018 - 2018 IEEE International Geoscience and Remote Sensing Symposium*, 7407–7410. <https://doi.org/10.1109/IGARSS.2018.8519255>
- m p rogers & associates pl. (2019). *Port Beach Coastal Adaptation Options - R1189 Rev 1*. https://www.fremantle.wa.gov.au/sites/default/files/Attachment%20under%20separate%20cover%20-%20OCM%20-%2011%20December%202019%20_0.pdf
- Naji, T., & Tawfeeq, R. (2011). Detection of Shoreline Change in AL-Thirthar Lake using Remotely Sensed Imagery and Topography Map. *IBN AL- HAITHAM J. FOR PURE & APPL. SCI.*, 24, 79–85.
- Pandian, P., Sethuraman, R., Murthy, M., Ramachandran, S., & Thayumanavan, S. (2009). Shoreline Changes and Near Shore Processes Along Ennore Coast, East Coast of South India. *Journal of Coastal Research*, 203, 828–845. [https://doi.org/10.2112/1551-5036\(2004\)20\[828:SCANSP\]2.0.CO;2](https://doi.org/10.2112/1551-5036(2004)20[828:SCANSP]2.0.CO;2)
- Pardo-Pascual, J. E., Almonacid-Caballer, J., Ruiz, L. A., & Palomar-Vázquez, J. (2012). Automatic extraction of shorelines from Landsat TM and ETM+ multi-temporal images with subpixel precision. *Remote Sensing of Environment*, 123, 1–11. <https://doi.org/10.1016/j.rse.2012.02.024>
- Seashore Engineering Pty Ltd. (2019). *Assessment of Coastal Erosion Hotspots in Western Australia Appendix D - Report SE052-01-Rev1*. https://www.transport.wa.gov.au/mediaFiles/marine/MAC_P_CoastalErosionHotspotsAppendixD135-191.pdf

- Stead, T. (2018). *Mapping Coastlines in WA Over 75 Years Capturing the Coastline*.
https://www.transport.wa.gov.au/mediaFiles/marine/MAC_P_CapturingtheCoastline.pdf
- Toffoli, A., & Bitner-Gregersen, E. M. (2017). Types of Ocean Surface Waves, Wave Classification. In *Encyclopedia of Maritime and Offshore Engineering* (pp. 1–8). John Wiley & Sons, Ltd.
<https://doi.org/10.1002/9781118476406.emoe077>
- Xu, H. (2006). Modification of normalised difference water index (NDWI) to enhance open water features in remotely sensed imagery. *International Journal of Remote Sensing*, 27(14), 3025–3033.
<https://doi.org/10.1080/01431160600589179>